

## Hadron structure after 25 years of QCD

A. W. Thomas<sup>a</sup>

<sup>a</sup> Department of Physics and Mathematical Physics and  
Special Research Centre for the Subatomic Structure of Matter,  
University of Adelaide, Australia 5005

We briefly review the status of our understanding of hadron structure based on QCD. This includes the role of symmetries, especially chiral symmetry, and the insights provided by lattice QCD. The main focus is on baryon structure and especially the nucleon, but this cannot be treated realistically without reference to spectroscopy. Our aim is to highlight recent insights and promising directions for future work.

### 1. INTRODUCTION

In the space allotted it is impossible to do justice to more than 40 years of work on hadron structure. Rather than attempt this, we take very seriously the appearance of QCD in the title and concentrate on the guidance that recent developments in our understanding of QCD provide for future developments in modelling hadron structure. For reviews of the vast amount of existing information on hadron models we refer to recent conferences on hadron structure.

In order to place hadron models firmly in the context of QCD, we begin with a summary of the properties of the non-perturbative vacuum, upon which everything else is built. We then recall some lessons from heavy quark systems before turning to the more complicated case of light quarks, where chiral symmetry plays a key role. We finish with a brief outlook concerning the theoretical and experimental possibilities in the next decade.

### 2. THE QCD VACUUM

It is by now firmly established that the ground state of QCD is a highly non-trivial state, including both quark and gluon condensates. For a purely gluonic version of QCD the vacuum energy density,  $\epsilon_{\text{vac}}$ , is:

$$\epsilon_{\text{vac}} = -\frac{9}{32} \langle 0 | \frac{\alpha_s}{\pi} G^2 | 0 \rangle = -0.5 \text{ GeV} / \text{fm}^3. \quad (1)$$

In comparison with phenomenological estimates of the energy difference between the perturbative and non-perturbative vacuum states, such as  $B$  in the MIT bag model, this is an

order of magnitude larger. Thus either the simple idea of the perturbative vacuum being fully restored inside a hadron is incorrect or the situation is rather more complicated than usually assumed.

The light quark condensates,  $\langle \bar{u}u \rangle$  and  $\langle \bar{d}d \rangle$ , in the non-perturbative vacuum are approximately equal and take a value around  $(-240 \text{ MeV})^3$ . A quantitative understanding of these values requires a treatment that in nuclear physics terms would involve at least Hartree-Fock plus RPA [1]. The underlying chiral symmetry of QCD (for massless  $u$  and  $d$  quarks) requires that, if the vacuum is to have a non-trivial quark condensate, there must be massless Goldstone bosons with the quantum numbers of the pion. As we move away from the massless limit, these Goldstone bosons have masses which behave as:

$$m_\pi^2 \propto \frac{\bar{m}_u + \bar{m}_d}{2} = \bar{m}. \quad (2)$$

(In fact, while this relation is only formally correct near  $\bar{m} = 0$ , lattice simulations show that it holds for  $m_\pi$  as large as 1 GeV.)

By studying the energy of two static sources of opposite color charge on a lattice, it has been shown that purely gluonic QCD leads to a linearly rising potential at large separations,  $V(R) = \sigma R$ . This observation naturally explains the observed Regge trajectories and effectively “confines” heavy color sources. Supplemented by a short-range, one-gluon exchange potential this naturally yields a potential of the Cornell type, which has proven phenomenologically so successful for heavy quark-anti-quark pairs:

$$V_{Q\bar{Q}}(r) = C - \frac{\alpha}{r} + \sigma r. \quad (3)$$

A linearly rising potential at large separations can be understood in terms of a non-perturbative vacuum which has dia-electric properties. By analogy with the Meissner effect in superconductors, one can think of the QCD vacuum containing a condensate of color magnetic monopoles which shield the lines of color electric force into a tube of constant cross section, no matter how far apart the color sources are located. Such a picture is supported by lattice simulations involving Abelian projection, but the final details are not yet settled [2]. On the other hand, in the real world this situation is altered dramatically by the presence of light quarks which can break the string once the energy stored becomes too great, through the process  $Q\bar{Q} \rightarrow Q\bar{q} + \bar{Q}q$  – e.g., for charm quarks,  $c\bar{c} \rightarrow D\bar{D}$ . For mesons which are stable under strong interactions, virtual processes like this have a quantitative effect – e.g.,  $f_B = 220 \text{ MeV}$  in quenched QCD (QQCD), whereas it is 260 MeV in full QCD – but do not change the qualitative picture [3].

## 2.1. Insights from lattice QCD

It has recently proven possible to compare various intermediate stages of lattice calculations, such as the quark and gluon propagators, with the forms commonly used in models. In this way one can refine the model building process using QCD itself. Of course, intermediate steps such as the quark and gluon propagators are not physical and one must specifically fix the gauge in order to make a meaningful comparison. The gauge most commonly used is Landau gauge and techniques have been developed to fix lattice quantities in this gauge. Figure 1 shows the result for the non-trivial momentum dependence of the gluon propagator (times  $q^2$ ) [4],  $q^2 D(q^2)$ , which should go to a constant at

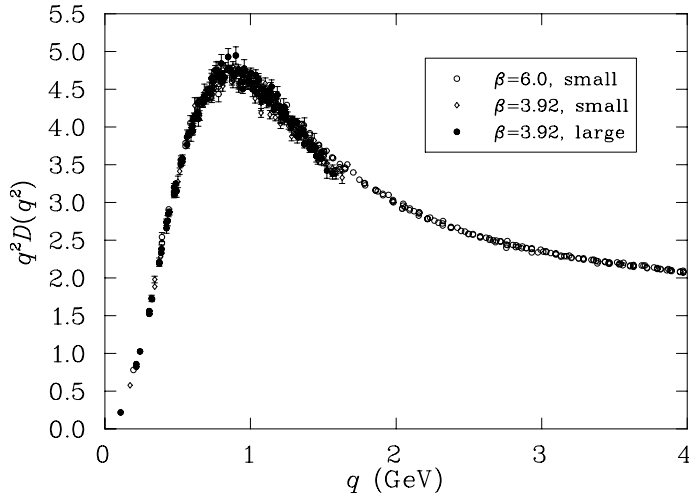


Figure 1. Non-perturbative behaviour of the gluon propagator (times  $q^2$ ) in Landau gauge, calculated from lattice QCD – from Ref. [4].

large  $q^2$  (up to perturbative QCD logs). From Fig. 1 we see that the lattice simulation shows that the gluon propagator is clearly *non-perturbative* for  $q^2 < 4\text{GeV}^2$ . Even more interesting from the point of view of model building is the fact that the gluon propagator is not enhanced as  $q^2 \rightarrow 0$ . While this agrees with some recent Schwinger-Dyson studies of QCD [5], it is in disagreement with at least a naive interpretation of a great deal of phenomenological work related to dynamical chiral symmetry breaking within the Schwinger-Dyson formalism [8]. Clearly this sort of interplay between phenomenological models and QCD itself has just begun and we have a great deal to learn from it.

Again with Landau gauge fixing, there have been some preliminary studies of the quark propagator in QCD. For Euclidean  $p^2$  one can write the quark propagator as:

$$S_E(p) = \frac{Z(p^2)}{i\gamma^\mu p_\mu + M(p^2)}. \quad (4)$$

The lattice simulations, which have so far been carried out with relatively large current quark masses, show a clear enhancement in the infrared [6,7]. For example, for a current quark mass of order 110 MeV, the simulations suggest  $M(0) \sim 400$  MeV, decreasing to around 300 MeV in the chiral limit. This is certainly consistent with the general idea of the constituent quark model and indeed this result provides a firm theoretical foundation for the concept within QCD. Of course, it also indicates where the concept breaks down and it is clear that in processes involving significant momentum transfer it will be necessary to go beyond the simple idea of a fixed mass. The similarity of the mass function,  $M(p^2)$ , to that found in Schwinger-Dyson studies [9] suggests that the latter may be a promising phenomenological extension of the constituent quark idea.

### 3. NON-RELATIVISTIC QUARK MODEL

The non-relativistic quark model, which combines the concept of a massive constituent quark with a linear, pairwise confining interaction and a short distance, spin-dependent hyperfine interaction, has had enormous success in correlating a vast amount of hadronic data. It provides an excellent basis for understanding the spectrum of mesons and baryons. Most notably, it has also provided a very natural explanation of why some states expected in the naive quark model have *not* been seen yet [10]. While until now this explanation has seemed convincing, it has not been seriously tested experimentally. This is now in process of change with Jefferson Lab due to produce a tremendous quantity of new, high duty factor data.

Amongst the key issues confronting the simple quark model, we mention relativity, the spin-orbit problem and chiral symmetry. It is quite clear that the approximation that the constituent  $u, d$  and  $s$  quarks are non-relativistic cannot be quantitatively reliable. For quarks of mass 300–400 MeV confined a volume of radius less than 1 fm, it is clear that  $p/M$  is of order one. The relativistic extension of the naive quark model, developed by Capstick, Isgur and others [11] has overcome this problem, with a resultant improvement in various transition form factors.

The spin-orbit problem has been around since the beginnings of the quark model, but has been of considerable interest recently in the light of claims that pseudoscalar meson exchange, rather than gluon exchange, as a source of hyperfine splitting would resolve the problem [12]. On the other hand, as noted by Isgur [13], with a Lorentz scalar confining potential one will automatically have large spin-orbit forces. The spin-orbit force arising from the usual one gluon exchange interaction can cancel this in the meson spectrum but not in the baryon spectrum. Thus the spin-orbit problem for the baryon spectrum is still very much with us – see however Ref. [14].

As we have already seen in connection with the structure of the non-perturbative vacuum, chiral symmetry is expected to play a major role in determining hadron structure for light quarks. Unfortunately the constituent quark model destroys that symmetry rather badly. We shall turn to a specific discussion of the role of chiral symmetry later, but simply note here that a quantitative discussion of hadronic properties is not possible unless measures are taken to ensure that the theory respects chiral symmetry.

#### 3.1. Hybrids

In a more sophisticated treatment of hadron spectroscopy the simple linear confining potential in Eq.(3) may be replaced by a flux tube model. This has the advantage that the confining potential then becomes truly dynamical and in particular can be excited. Excitations of the flux tube can result in a new kind of hadron. The most interesting cases are those where the quantum numbers of the hadron are *exotic* – e.g., for mesons where they cannot be associated with a  $q\bar{q}$  system.

The experimental discovery of exotic systems, where the gluons have a genuine structural role, would be a vital step towards a full understanding of QCD. This explains the excitement over the announcement, from E852 at Brookhaven National Lab [15], of three candidates for hybrid mesons with quantum numbers  $J^{PC} = 1^{-+}$ . The  $\pi'(1370)$  was seen in the  $\pi\eta$  and  $\pi\eta'$  channels, the  $\pi'(1640)$  in  $\pi\eta', \rho\pi$  and  $f_1\pi$  and the  $\pi'(2000)$  in  $a_1\eta$ . These masses are somewhat lower than the values usually reported in lattice

simulations, although for the moment the latter tend to be based on quenched QCD [16]. While the interpretation of the BNL data should become clearer over the next few years, the announcement lends even greater urgency to the calls for a future HALL D program at Jefferson Lab.

### 3.2. Glueballs

An even more dramatic prediction of QCD than exotic states is, of course, the possibility of physical particles containing *only* glue – the glueballs. Lattice simulations suggest that the lowest mass state of pure glue would be the  $0^{++}$  with a mass of  $1670 \pm 20$  MeV [17]. Experimental searches have so far found a number of scalar glueball candidates in the mass region 1300 to 1800 MeV. However, the interpretation of the data is badly effected by the fact that in *real* QCD, with light quarks, no physical state will be pure glue – rather the best one can hope for is an unstable state with only a small  $q\bar{q}$  component for some (unknown) dynamical reason. We note that the channel coupling effects induced by decay channels such as  $\pi\pi$  and  $K\bar{K}$  are also quite controversial from the theoretical point of view. There is clearly room for a great deal of experimental and theoretical work in this field in the future, with a promise of fame and fortune for the unambiguous identification of a glueball state.

## 4. LIGHT QUARKS

As we have already explained, the vast majority of theoretical papers dealing with light quark systems have been based on the constituent quark model. This approach has achieved a great deal and, as we have seen in Sect. 2, there is a clear qualitative connection between this model and the properties of QCD revealed through lattice calculations. Nevertheless, the constituent quark model is better suited to dealing with systems of quarks that are genuinely heavy. Here we take the chiral properties of QCD very seriously, in order to explore the unique features of light quark systems.

### 4.1. Trace Anomaly

If one defines a tensor  $\mathcal{S}^\mu = x_\nu \theta^{\mu\nu}$ , with  $\theta^{\mu\nu}$  the energy-momentum tensor of QCD, one finds classically that  $\partial_\mu \mathcal{S}^\mu$  is zero. However, if this were to hold at the quantum level we would find that the nucleon mass would be zero. Fortunately the divergence of  $\mathcal{S}^\mu$  is no longer zero in quantum field theory because of the trace anomaly and one finds for the nucleon mass:

$$M_N = \langle N | -\frac{9}{4}\alpha_s \text{Tr}G^2 + m_u \bar{u}u + m_d \bar{d}d + m_s \bar{s}s | N \rangle. \quad (5)$$

By far the dominant term on the rhs of Eq.(5) is the gluon trace [18]. (The  $u$  and  $d$  quark mass terms are known to be of order 40-50 MeV from the sigma commutator and while the  $s$ -quark mass term is less well known its not more than 100 MeV or so.)

A full understanding of hadron structure in terms of QCD must involve a reasonable physical interpretation of Eq. (5). For the present it is clear that the nucleon mass arises from non-perturbative gluon interactions and that is certainly reflected there. There are many famous examples of virial theorems which relate apparently different physical quantities and it is likely that such a theorem connects the effective or constituent quark mass appearing in Eq. (4) to the gluon field energy in Eq. (5).

## 4.2. QCD Sum Rules

The QCD sum rules have had considerable success in relating hadron masses to various properties of the non-perturbative vacuum. The famous Ioffe formula for the nucleon mass [19]:

$$M_N = -\frac{8\pi^2}{\mathcal{M}^2} \langle \bar{q}q \rangle, \quad (6)$$

yields a surprisingly accurate value provided the Borel mass  $\mathcal{M}$  is taken to be about 1 GeV. It also illustrates clearly the role of the quark condensate in generating a chiral symmetry violating property such as mass. On the other hand, the connection to Eq. (5) is totally unclear. More important, the dependence on  $\langle \bar{q}q \rangle$  is incorrect compared with what is found if higher order condensates are included [20]. In addition, the leading non-analytic chiral behaviour of the left and right hand sides of Eq. (6) are inconsistent.

## 4.3. Quenched Lattice QCD

Perhaps the most impressive non-perturbative results for the spectrum of light hadrons has been obtained using quenched lattice QCD. Once the lattice scale (i.e. the lattice spacing,  $a$ ) is set by fitting one mass – either that of the  $\rho$  or  $\phi$  meson – the other ground state meson and baryon masses agree with experiment within about 10% [21]. This is a remarkable result, even though one would rather set  $a$  using the string tension, in which case all the masses would be genuine predictions. On the other hand, the success raises as many questions as it resolves. Since the chiral properties of quenched QCD (QQCD) are quite different from those of full QCD [22], it becomes vital to understand how one can, nevertheless, obtain such spectacular agreement. Unfortunately, it will not be possible to handle realistic light quark masses for sea quarks (i.e. in quark loops) for quite a few years yet. However, it is known that chiral symmetry plays a vital role in hadron structure and we have some clues as to how it might effect lattice calculations.

## 4.4. Non-Analytic Behaviour

We have already seen that spontaneous chiral symmetry breaking in QCD requires the existence of Goldstone bosons whose masses vanish in the limit of zero quark mass (the chiral limit). As a corollary to this, there must be contributions to hadron properties from Goldstone boson loops. These loops have the unique property that they give rise to terms in an expansion of most hadronic properties as a function of quark mass which are not analytic. As a simple example, consider the nucleon mass. The most important chiral corrections to  $M_N$  come from the processes  $N \rightarrow N\pi \rightarrow N$  ( $\sigma_{NN}$ ) and  $N \rightarrow \Delta\pi \rightarrow N$  ( $\sigma_{N\Delta}$ ). (We will come to what it means to say these are the most important shortly.) We write  $M_N = M_N^{\text{bare}} + \sigma_{NN} + \sigma_{N\Delta}$ . In the heavy baryon limit one has

$$\sigma_{NN} = -\frac{3g_A^2}{16\pi^2 f_\pi^2} \int_0^\infty dk \frac{k^4 u^2(k)}{k^2 + m_\pi^2}. \quad (7)$$

Here  $u(k)$  is a natural high momentum cut-off which is the Fourier transform of the source of the pion field (e.g. in the cloudy bag model (CBM) it is  $3j_1(kR)/kR$ , with  $R$  the bag radius [23]). From the point of view of PCAC it is natural to identify  $u(k)$  with the axial form-factor of the nucleon, a dipole with mass parameter  $1.02 \pm 0.08\text{GeV}$ .

Quite independent of the form chosen for the ultra-violet cut-off, one finds that  $\sigma_{NN}$  is a non-analytic function of the quark mass. The non-analytic piece of  $\sigma_{NN}$  is independent of the form factor and gives

$$\sigma_{NN}^{LNA} = -\frac{3g_A^2}{32\pi f_\pi^2} m_\pi^3 \sim \bar{m}^{\frac{3}{2}}. \quad (8)$$

This has a branch point, as a function of  $\bar{m}$ , at  $\bar{m} = 0$ . Such terms can only arise from Goldstone boson loops.

#### 4.5. Chiral Extrapolations of Lattice Data

It is natural to ask how significant this non-analytic behaviour is in practice. If the pion mass is given in GeV,  $\sigma_{NN}^{LNA} = -5.6m_\pi^3$  and at the physical pion mass it is just -17 MeV. However, at only three times the physical pion mass,  $m_\pi = 420\text{MeV}$ , it is -460MeV – half the mass of the nucleon. If one's aim is to extract physical nucleon properties from lattice QCD calculations this is extremely important. The most sophisticated lattice calculations with dynamical fermions are only just becoming feasible at such low masses and to connect to the physical world one must extrapolate from  $m_\pi \sim 500\text{MeV}$  to  $m_\pi = 140\text{MeV}$ . Clearly one must have control of the chiral behaviour.

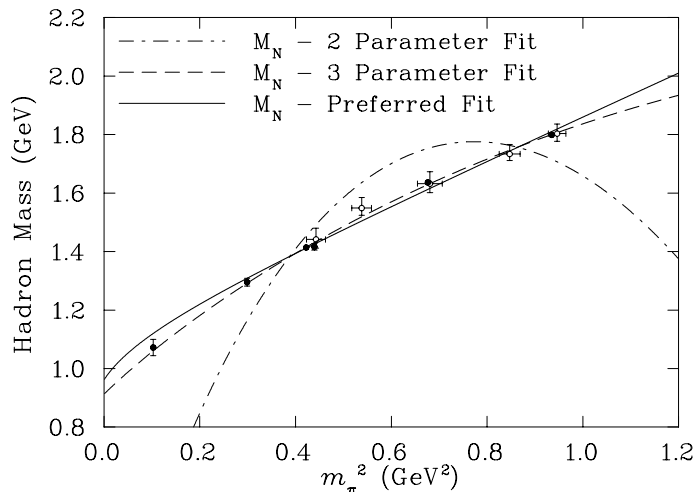


Figure 2. A comparison between phenomenological fitting functions for the mass of the nucleon – from Ref. [25]. The two parameter fit corresponds to using Eq.(9) with  $\gamma$  set equal to the value known from  $\chi$ PT. The three parameter fit corresponds to letting  $\gamma$  vary as an unconstrained fit parameter. The solid line is the two parameter fit based on the functional form of Eq.(10).

Figure 2 shows recent lattice calculations of  $M_N$  as a function of  $m_\pi^2$  from CP-PACS and UKQCD [24]. The dashed line indicates a fit which naively respects the presence of a LNA term,

$$M_N = \alpha + \beta m_\pi^2 + \gamma m_\pi^3, \quad (9)$$

with  $\alpha, \beta$  and  $\gamma$  fitted to the data. While this gives a very good fit to the data, the chiral coefficient  $\gamma$  is only -0.761, compared with the value -5.60 required by chiral symmetry. If one insists that  $\gamma$  be consistent with QCD the best fit one can obtain with this form is the dash-dot curve. This is clearly unacceptable.

An alternative suggested recently by Leinweber et al. [25], which also involves just three parameters, is to evaluate  $\sigma_{NN}$  and  $\sigma_{N\Delta}$  with the same ultra-violet form factor, with mass parameter  $\Lambda$ , and to fit  $M_N$  as

$$M_N = \alpha + \beta m_\pi^2 + \sigma_{NN}(m_\pi, \Lambda) + \sigma_{N\Delta}(m_\pi, \Lambda). \quad (10)$$

Using a sharp cut-off ( $u(k) = \theta(\Lambda - k)$ ) these authors were able to obtain analytic expressions for  $\sigma_{NN}$  and  $\sigma_{N\Delta}$  which reveal the correct LNA behaviour – and next to leading (NLNA) in the  $\Delta\pi$  case,  $\sigma_{N\Delta}^{NLNA} \sim m_\pi^4 \ln m_\pi$ . These expressions also reveal a branch point at  $m_\pi = M_\Delta - M_N$ , which is important if one is extrapolating from large values of  $m_\pi$  to the physical value. The solid curve in Fig. 2 is a two parameter fit to the lattice data using Eq.(10), but fixing  $\Lambda$  at a value suggested by CBM simulations to be equivalent to the preferred 1 GeV dipole. A small increase in  $\Lambda$  is necessary to fit the lowest mass data point, at  $m_\pi^2 \sim 0.1 \text{ GeV}^2$ , but clearly one can describe the data very well while preserving the exact LNA and NLNA behaviour of QCD.

#### 4.6. The Sigma Commutator

The analysis of the lattice data for  $M_N$ , incorporating the correct non-analytic behaviour, can yield interesting new information concerning the sigma commutator of the nucleon:

$$\sigma_N = \frac{1}{3} \langle N | [Q_{i5}, [Q_{i5}, H_{QCD}]] | N \rangle = \langle N | \bar{m}(\bar{u}u + \bar{d}d) | N \rangle. \quad (11)$$

This is a direct measure of chiral SU(2) symmetry breaking in QCD, and the widely accepted experimental value is  $45 \pm 8 \text{ MeV}$  [26]. (Although there are recent suggestions that it might be as much as 20 MeV larger [27].) Using the Feynman-Hellmann theorem one can also write

$$\sigma_N = \bar{m} \frac{\partial M_N}{\partial \bar{m}} = m_\pi^2 \frac{\partial M_N}{\partial m_\pi^2}. \quad (12)$$

Historically, lattice calculations have evaluated  $\langle N | (\bar{u}u + \bar{d}d) | N \rangle$  at large quark mass and extrapolated this scale dependent quantity to the “physical” quark mass, which had to be determined in a separate calculation. The latest result with dynamical fermions,  $\sigma_N = 18 \pm 5 \text{ MeV}$  [28], illustrates how difficult this procedure is. On the other hand, if one has a fit to  $M_N$  as a function of  $m_\pi$  which is consistent with chiral symmetry, one can evaluate  $\sigma_N$  directly using Eq.(12). Using Eq.(10) with a sharp cut-off yields  $\sigma_N \sim 55 \text{ MeV}$ , while a dipole form gives  $\sigma_N \sim 45 \text{ MeV}$  [29]. The residual model dependence can only be removed by more accurate lattice data at low  $m_\pi^2$ . Nevertheless, the result  $\sigma_N \in (45, 55) \text{ MeV}$  is in very good agreement with the data. In contrast, the simple cubic fit, with  $\gamma$  inconsistent with chiral constraints, gives  $\sim 30 \text{ MeV}$ . Until the experimental situation regarding  $\sigma_N$  improves, it is not possible to draw definite conclusions regarding the strangeness content of the nucleon [30] from this analysis, but the fact that two-flavour QCD reproduces the current preferred value should certainly stimulate more work.



#### 4.7. A Caution

A number of chiral constituent quark models are in common use, which involve a Hamiltonian with a pairwise, static one-pion-exchange force between quarks. It is important to realise that such models cannot be consistent with the general chiral constraints of QCD. By including only pairwise pion-exchange interactions, one is omitting Goldstone loops in which the pion is emitted and absorbed by the same quark [31]. It is a simple exercise to convince oneself that all diagrams, including any number of Goldstone boson loops, gluon exchanges and so on, provided they can be cut on a single pion line, can be exactly written as  $\sum_B \sigma_{NB}$ . Like  $\sigma_{NN}$  and  $\sigma_{N\Delta}$ ,  $\sigma_{NB}$  describes the process  $N \rightarrow B\pi \rightarrow N$ , with a renormalized  $\pi NB$  vertex at each end of the pion loop.

The LNA behaviour of  $M_N$  comes from  $B = N$ , because only this is degenerate with the initial nucleon. The NLNA behaviour comes from  $B = \Delta$ , because this is the lowest mass baryon excitation available.  $\sigma_{NN}$  and  $\sigma_{N\Delta}$  are the most important chiral corrections because they produce the LNA and NLNA behaviour. Heavier intermediate states will produce only relatively slow variations of  $M_N$  with  $m_\pi$  and can be summed phenomenologically into  $\alpha$  and  $\beta$  in Eq.(9). This was the procedure advocated in the CBM [23] and we see that it is completely consistent with the chiral behaviour of QCD and chiral perturbation theory, in particular.

We stress that in order to ensure the correct chiral behaviour of hadron properties one must include all Goldstone loops, including those where it is emitted and absorbed by the same quark. While it is tempting to argue that the boson loop on the same quark could be included in the constituent quark mass, this is incorrect. Whether one gets LNA or NLNA behaviour depends on the environment in which the quark finds itself. For the nucleon case, if the intermediate quark plus its spectators has  $J = \frac{3}{2}$  it is NLNA, while if the three quarks form a nucleon it is LNA. *There is no alternative but to consistently evaluate Goldstone boson loops at the hadronic level.*

#### 4.8. Baryon Electromagnetic Properties

It is a completely general consequence of quantum mechanics that the long-range charge structure of the proton comes from its  $\pi^+$  cloud ( $p \rightarrow n\pi^+$ ), while for the neutron it comes from its  $\pi^-$  cloud ( $n \rightarrow p\pi^-$ ). However it is not often realized that the LNA contribution to the nucleon charge radius goes like  $\ln m_\pi$  and diverges as  $\bar{m} \rightarrow 0$  [33]. This can never be described by a constituent quark model. Figure 3 shows the latest data from Mainz and Nikhef for the neutron electric form factor, in comparison with CBM calculations for a confinement radius between 0.9 and 1.0 fm. The long-range  $\pi^-$  tail of the neutron plays a crucial role.

The situation for baryon magnetic moments is also very interesting. The LNA contribution in this case arises from the diagram where the photon couples to the pion loop. As this involves two pion propagators the expansion of the proton and neutron moments is:

$$\mu^{p(n)} = \mu_0^{p(n)} \mp \alpha m_\pi + \mathcal{O}(m_\pi^2). \quad (13)$$

Here  $\mu_0^{p(n)}$  is the value in the chiral limit and the linear term in  $m_\pi$  is proportional to  $\bar{m}^{\frac{1}{2}}$ , a branch point at  $\bar{m} = 0$ . The coefficient of the LNA term is  $\alpha = 4.4\mu_N - \text{GeV}^{-1}$ . At the physical pion mass this LNA contribution is  $0.6\mu_N$ , which is almost a third of the neutron

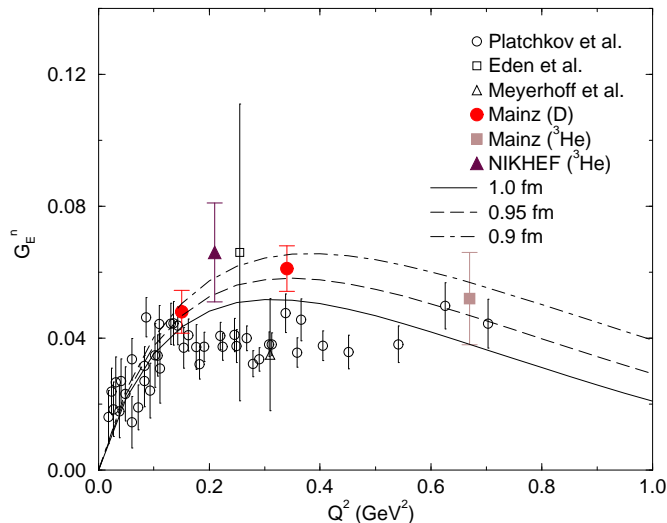


Figure 3. Recent data for the neutron electric form factor in comparison with CBM calculations for a confining radius around 0.95fm – from Ref. [32].

magnetic moment. *No constituent quark model can or should get better agreement with data than this.*

Just as for  $M_N$ , the chiral behaviour of  $\mu^{p(n)}$  is vital to a correct extrapolation of lattice data. One can obtain a very satisfactory fit to some rather old data, which happens to be the best available, using the simple Padé [34]:

$$\mu^{p(n)} = \frac{\mu_0^{p(n)}}{1 \pm \frac{\alpha}{\mu_0^{p(n)}} m_\pi + \beta m_\pi^2} \quad (14)$$

The data can only determine two parameters and Eq.(14) has just two free parameters while guaranteeing the correct LNA behaviour as  $m_\pi \rightarrow 0$  **and** the correct behaviour of HQET at large  $m_\pi^2$ . The extrapolated values of  $\mu^p$  and  $\mu^n$  at the physical pion mass,  $2.85 \pm 0.22 \mu_N$  and  $-1.90 \pm 0.15 \mu_N$  are currently the best estimates from non-perturbative QCD [34]. For more details of this fit and the application of similar ideas to other members of the nucleon octet, as well as the strangeness magnetic moment of the nucleon, we refer to the presentation of D. Leinweber at this conference [35].

#### 4.9. Deep-Inelastic Scattering

Although deep inelastic scattering has predominantly been used as a testing ground for perturbative QCD, the parton distributions contain direct information on the energy-momentum distribution of quarks and gluons inside the hadron. This is vital to our understanding of how hadron structure is realized in non-perturbative QCD. Of course, this information is viewed in a particular frame of reference, the infinite momentum frame. The problem of zero modes on in light-cone field theory is widely appreciated and the

chiral behaviour of hadronic properties is usually believed to be part of that general problem. However, the LNA behaviour of these properties can give us some insight.

The observation that non-analytic behaviour in  $\bar{m}$  can only come from Goldstone boson loops is just as true on the light-cone as anywhere else. Consider the process  $N \rightarrow N\pi \rightarrow N$  in light-cone field theory. It is a straightforward exercise to show that the expression obtained using the Feynman rules for light-cone field theory does indeed have the LNA behaviour required by QCD. This seems natural, why bother to mention it? The point is that this LNA behaviour can only come from a  $\pi N$  intermediate state. The subtle correlations in the pion which guarantee that  $m_\pi^2 \propto \bar{m}$ , vanishing in the chiral limit, must be included. One will *never* obtain the LNA behaviour by including a few or even quite a lot of leading Fock components in the nucleon wavefunction.

This simple argument leads us to conclude that both  $N\pi$  and  $\Delta\pi$  Fock components must be incorporated in the light-cone wave function of the nucleon if one is satisfy chiral constraints. One now famous consequence of this is the excess of  $\bar{d}$  over  $\bar{u}$  quarks in the proton, predicted [36] in 1983 and observed by NMC in 1990 [37]. This measurement, and the important developments since then [38], have given us vital new information about the non-perturbative chiral structure of the nucleon. In this light it satisfying to see the remarkable result recently obtained by Melnitchouk et al. [39], which relates the LNA behaviour of the excess of  $\bar{d}$  over  $\bar{u}$  quarks to the LNA behaviour of the nucleon wave function renormalization constant:

$$\int_0^1 dx (\bar{d}(x) - \bar{u}(x)) |_{LNA} \sim m_\pi^2 \ln m_\pi. \quad (15)$$

## 5. Future Challenges in Spectroscopy

The calculation of the properties of highly excited baryons within lattice QCD is a very difficult challenge. However, for the lowest negative parity states new techniques have been developed which seem very promising [40]. On the experimental side we can expect a tremendous wealth of new data from Jefferson Lab in the next few years. This should greatly clarify the situation regarding “missing states” and give us a much clearer picture concerning many other resonances.

One of the major theoretical challenges for the near future is the need to deal with the coupling of hadron resonances to various meson-baryon channels (open and closed). Not only do we have a problem that some states expected in the quark model are missing but there may be other states that should not be considered quark states at all. A famous example is the  $\Lambda(1405)$ , which almost certainly results from the extremely strong attraction in the  $\Sigma\pi$  s-wave, coupled to  $\bar{K}N$  [41]. Another candidate which has attracted a great deal of theoretical attention is the Roper. The most recent study by the Jülich group, including the effect of coupled  $\pi N$ ,  $\pi\Delta$  and  $\sigma N$  channels, strongly suggests that the Roper is not a quark model state [42]. This would certainly resolve a number of problems with its low mass.

While these interpretations of the  $\Lambda(1405)$  and the Roper seem to be correct, there is a real danger in an uncontrolled coupled channels approach to such problems. As illustrated by the classic case of the Chew-Low model of the  $\Delta(1232)$ , it is always possible to generate a resonance through multiple scattering. On the other hand, we know that

in the absence of open channels QCD predicts the existence of hadrons. It is essential in unravelling the nature of observed resonance states that one must use a consistent model of the internal structure of the hadrons involved in order to calculate the appropriate coupling to relevant meson-baryon channels. The classic CBM work on the  $\Delta(1232)$  showed that in such an approach it was clear that it is primarily a three-quark state, not the result of strong pion-nucleon rescattering. The Jülich group finds a similar result for the  $S_{11}(1535)$  – even though its coupling to  $\eta N$  is very strong. Finally, we note that while the examples quoted have been baryon resonances, exactly the same questions arise for mesons [43]. This is a field of study which is just beginning in earnest.

## 6. Conclusion

It is clear that there have been some outstanding developments in our understanding of hadron structure in terms of QCD over the last 25 years. Yet the next 10 promise much more. We can expect data on hadron electroweak form factors of increasing precision over a vastly wider range of kinematic variables. We can also expect an entirely new range of observables, including for the nucleon: virtual Compton scattering (VCS), deeply VCS, spin-dependent Compton scattering, transition form factors to (and between) new baryon resonances, determinations of  $G_E^s$  and  $G_M^s$ , the nucleon anapole moment and semi-inclusive deep-inelastic scattering data.

On the theoretical side there will be rapid progress in lattice QCD, with improved actions and faster computers making it possible to include dynamical quarks with masses approaching the physical region. Improved interaction between phenomenology and lattice simulations will lead to ever more reliable chiral extrapolations of the physical properties of hadrons. There will also be serious and consistent studies of the effects of channel coupling, both for regular meson and baryon resonances but also for hybrids and glueballs. Finally, we can expect a great deal more productive feedback between the results of QCD inspired models and lattice simulations.

## ACKNOWLEDGEMENTS

It is a pleasure to acknowledge the collaboration and helpful discussions with many staff, students and visitors at the CSSM who have contributed to my understanding of the problems discussed here, especially C. Boros, G. Krein, D. Leinweber, D. Lu, W. Melnitchouk, F. Steffens, K. Tsushima, A. Williams and S. Wright. This work was supported by the Australian Research Council and the University of Adelaide.

## REFERENCES

1. F. J. Llanes-Estrada and S. R. Cotanch, Phys. Rev. Lett. **84** (2000) 1102.
2. Y. Koma, H. Suganuma, K. Amemiya, M. Fukushima and H. Toki, hep-ph/9912347.
3. C. Bernard *et al.*, hep-lat/0002028.
4. F. D. Bonnet *et al.*, hep-lat/0002020.
5. R. Alkofer and L. von Smekal, to appear in Nucl. Phys., hep-ph/0004141.
6. J. I. Skullerud and A. G. Williams, Nucl. Phys. Proc. Suppl. **83-84** (2000) 209.
7. S. Aoki *et al.* [JLQCD Collaboration], Phys. Rev. Lett. **82** (1999) 4392.

8. F. T. Hawes *et al.*, Phys. Lett. **B440** (1998) 353 [nucl-th/9807056].
9. C. D. Roberts and A. G. Williams, Prog. Part. Nucl. Phys. **33** (1994) 477.
10. N. Isgur and G. Karl, Phys. Rev. **D18** (1978) 4187.
11. S. Capstick and N. Isgur, Phys. Rev. **D34** (1986) 2809.
12. L. Y. Glozman and D. O. Riska, Phys. Rept. **268** (1996) 263 [hep-ph/9505422].
13. N. Isgur, nucl-th/9908028.
14. L. Y. Glozman, nucl-th/9909021.
15. G. S. Adams *et al.* [E852 Collaboration], Phys. Rev. Lett. **81** (1998) 5760.
16. P. Lacock *et al.* [UKQCD Collaboration], Phys. Rev. **D54** (1996) 6997.
17. C. Michael, Nucl. Phys. **A655** (1999) 12 [hep-ph/9810415].
18. X. Ji, Phys. Rev. Lett. **74** (1995) 1071 [hep-ph/9410274].
19. B. Ioffe, Nucl. Phys. **188** (1978) 317
20. D. B. Leinweber, Annals Phys. **254** (1997) 328 [nucl-th/9510051].
21. S. Aoki *et al.* [CP-PACS Collaboration], Phys. Rev. Lett. **84** (2000) 238.
22. J. N. Labrenz and S. R. Sharpe, Phys. Rev. **D54** (1996) 4595 [hep-lat/9605034].
23. S. Theberge, A. W. Thomas and G. A. Miller, Phys. Rev. **D22** (1980) 2838; A. W. Thomas, Adv. Nucl. Phys. **13** (1984) 1.
24. S. Aoki *et al.* [CP-PACS-Collaboration], Phys. Rev. **D60** (1999) 114508 ; C. R. Allton *et al.* [UKQCD Collaboration], Phys. Rev. **D60** (1999) 034507 .
25. D. B. Leinweber *et al.*, Phys. Rev. **D61** (2000) 074502 [hep-lat/9906027].
26. J. Gasser, H. Leutwyler and M. E. Sainio, Phys. Lett. **B253**, 252 (1991).
27. M. Knecht, hep-ph/9912443.
28. **SESAM** Collaboration, S. Gusken *et al.*, Phys. Rev. **D59**, 054504 (1999).
29. D. B. Leinweber *et al.*, Phys. Lett. **B482** (2000) 109 [hep-lat/0001007].
30. J. Ellis, in Proc. this conference, hep-ph/0005322.
31. A. W. Thomas and G. Krein, Phys. Lett. **B456** (1999) 5 [nucl-th/9902013].
32. D. H. Lu *et al.*, in Proc. this conference; D. H. Lu *et al.*, Phys. Rev. **C60** (1999) 068201 [nucl-th/9807074].
33. D. B. Leinweber and T. D. Cohen, Phys. Rev. **D47** (1993) 2147 [hep-lat/9211058].
34. D. B. Leinweber *et al.*, Phys. Rev. **D60** (1999) 034014 [hep-lat/9810005].
35. D. B. Leinweber and A. W. Thomas, in Proc. this conference.
36. A. W. Thomas, Phys. Lett. **B126** (1983) 97.
37. P. Amaudruz *et al.* [New Muon Collaboration], Phys. Rev. Lett. **66** (1991) 2712.
38. E. A. Hawker *et al.* [NuSea Collaboration], Phys. Rev. Lett. **80** (1998) 3715.
39. A. W. Thomas, W. Melnitchouk and F. M. Steffens, hep-ph/0005043.
40. F. X. Lee and D. B. Leinweber, Nucl. Phys. Proc. Suppl. **73** (1999) 258.
41. N. Kaiser, P. B. Siegel and W. Weise, Nucl. Phys. **A594** (1995) 325 [nucl-th/9505043]; E. A. Veit *et al.*, Phys. Rev. **D31** (1985) 1033; R. H. Dalitz and A. Deloff, J. Phys. G **G17** (1991) 289.
42. C. Schutz *et al.*, Phys. Rev. **C57** (1998) 1464.
43. D. Cabrera, E. Oset and M. J. Vicente-Vacas, nucl-th/0006029.